Eur Radiol (2011) 21: 26–35
DOI 10.1007/s00330-010-1897-1

CARDIAC

Sung Min Ko
Jin Woo Choi
Meong Gun Song
Je Kyoun Shin
Hyun Kun Chee
Hyun Woo Chung
Dong Hun Kim

Myocardial perfusion imaging using adenosine-induced stress dual-energy computed tomography of the heart: comparison with cardiac magnetic resonance imaging and conventional coronary angiography

Received: 5 February 2010
Accepted: 21 June 2010
Published online: 25 July 2010

S. M. Ko (✉) · J. W. Choi
Department of Radiology,
Konkuk University Hospital,
Konkuk University School of Medicine,
4-12 Hwayang-dong, Gwangjin-gu,
Seoul, 143-729, Korea
e-mail: ksm9723@yahoo.co.kr
Tel.: +82-2-20305578
Fax: +82-2-4478726

M. G. Song · J. K. Shin · H. K. Chee
Department of Thoracic surgery,
Konkuk University Hospital,
Konkuk University School of Medicine,
Seoul, Korea

H. W. Chung
Department of Nuclear medicine,
Konkuk University Hospital,
Konkuk University School of Medicine,
Seoul, Korea

D. H. Kim
Department of Radiology,
Soonchunhyang University Bucheon
Hospital, Soonchunhyang University,
College of Medicine, Seoul, Korea

Abstract *Objective* To evaluate the feasibility and diagnostic accuracy of adenosine-stress dual-energy computed tomography (DECT) for detecting haemodynamically significant stenosis causing reversible myocardial perfusion defect (PD) compared with stress perfusion magnetic resonance imaging (SP-MRI) and conventional coronary angiography (CCA). *Methods* Fifty patients with known coronary artery disease (CAD) detected by dual-source CT (DSCT) were investigated by contrast-enhanced, stress DECT with high- and low-energy x-ray spectra settings during adenosine infusion. A colour-coded iodine map was used for evaluation of myocardial PDs compared with rest DSCT perfusion images. Reversible myocardial PDs according to the stress DECT/rest DSCT were compared with SP-MRI on a segmental basis and CCA on a vascular territorial basis. *Results* A total of 697 myocardial segments and 123 vascular territories of 41 patients were analysed. Three hundred one segments and 72 vascular territories in 38 patients showed reversible PDs on stress DECT. Stress DECT had 89% sensitivity, 78% specificity and 82% accuracy for detecting segments with reversible PDs seen on SP-MRI (n=28). Compared with CCA (n=41), stress DECT had 89% sensitivity, 76% specificity and 83% accuracy for the detection of vascular territories with reversible myocardial PDs that had haemodynamically relevant CAD. *Conclusion* Adenosine stress DECT can identify stress-induced myocardial PD in patients with CAD.

Keywords Computed tomography (CT) · Coronary artery disease · Dual-energy CT · Ischaemia · Myocardial perfusion

Introduction

A myocardial perfusion abnormality occurs before left ventricular (LV) wall motion abnormality or electrocardiography (ECG) changes in the ischaemic cascade [1, 2]. The haemodynamic relevance of known coronary stenoses can be assessed by the presence, extent and severity of a pharmacologically induced stress perfusion defect (PD) using myocardial perfusion imaging (MPI) by single photon emission computed tomography (SPECT), positron emission tomography and cardiac magnetic resonance imaging (MRI). MPI has been proven to be a useful and reliable method for the diagnosis and risk stratification of patients with coronary artery disease (CAD) [3, 4].

Animal models and preliminary human studies of adenosine-induced stress (AIS) computed tomography (CT) have shown that CT can depict ischaemic myocardium that is supplied by a significant coronary stenosis, and the findings agree with those for SPECT and conventional coronary angiography (CCA) [5–8]. However, MPI using CT requires high temporal resolution to reduce cardiac motion artefacts caused by the increased heart rate (HR) during adenosine infusion and a method for low-

ering patient radiation exposure. Dual-source CT (DSCT) with two x-ray tubes and two corresponding detectors arrays mounted in the same gantry has high temporal resolution of 83 ms and pitch adaptation [9]. With AIS-DSCT, coronary artery morphology and myocardial perfusion abnormality can be assessed simultaneously [10]. Recent studies using DSCT with dual-energy mode ["dual-energy CT" [DECT]] have shown that contrast-enhanced DECT has the potential to assess changes in the status of myocardial perfusion for computing iodine distribution within the myocardium [11–14]. Even though these studies demonstrated reproducible detection of myocardial ischaemia, further multicentre research is required for the validation of the diagnostic value of DECT for assessing myocardial perfusion.

There are few published studies on the detection of myocardial ischaemia using AIS-DECT. We hypothesised that AIS-DECT can detect reversible PDs in myocardial areas of normal resting perfusion that are supplied by haemodynamically significant coronary stenoses. Thus, the purpose of our study was to evaluate the feasibility and diagnostic accuracy of AIS-DECT for detecting haemodynamically significant stenosis causing reversible myocardial PD compared with stress perfusion (SP) MRI and CCA.

Materials and methods

Study population

This study was conducted prospectively, enrolling 50 consecutive patients (20 women, 30 men; mean age 64.6± 9 years; range 46-75 years) with documented CAD that was diagnosed by using DSCT coronary angiography (CA). Reasons for DSCT-CA examination were typical or atypical chest pain, pathological treadmill test or dyspnea. All patients were scheduled for CCA and were asked to undergo AIS-DECT. They had been clinically referred for MPI using SP-MRI to further evaluate the AIS-DECT results in the context of known CAD. Reasons for exclusion included previous percutaneous coronary intervention or coronary artery bypass graft, severe arrhythmia, unstable clinical status, acute coronary syndrome, old myocardial infarction (MI), asthma, critical aortic stenosis, deteriorated renal function (serum creatinine >1.5 mg/dl), congestive heart failure of New York Heart Association class IV, greater than first degree atrio-ventricular block and contraindication to cardiac MRI (incompatible metallic implants, claustrophobia). The study protocol was approved by the institutional ethics committee, and all patients gave written informed consent before enrolment.

Image acquisition

AIS-DECT Patients were instructed not to drink coffee or tea and not to have oral beta-blockers for at least 24 h before the DECT. Two intravenous lines were inserted (18 gauge for contrast medium delivery; 20 gauge for adenosine infusion). Before the examination, the HR of each patient was measured. Beta-blockers and nitroglycerine were not used in order to avoid impact on myocardial perfusion. All CT examinations were performed on DSCT (Somatom Definition, Siemens Medical Solutions, Forchheim, Germany) in dual-energy mode. DECT was performed using the following imaging parameters: 330 ms gantry rotation time, heart rate adaptive pitch of 0.2–0.43, 32×2×0.6-mm collimation with z-flying focal spot technique and 165 ms temporal resolution. One tube of the DSCT was operated with 82 mAs/rotation at 140 kV, the second tube with 164 mAs/rotation at 80 kV. Blood pressure, standard ECG and clinical symptoms were carefully monitored during the adenosine infusion and after imaging.

With the scout image, the anatomical range extended from 2 cm below the level of the tracheal bifurcation to the diaphragm in a craniocaudal direction. Adenosine infusion was started at a constant rate of 140 μg/kg/min over 6 min. Retrospectively gated imaging with ECG-based tube current modulation (Mindose) and pitch adaptation was obtained 4 min after the initiation of the adenosine infusion. We used tube current modulation with MinDose in all patients. Full tube current was applied from 60–75% of the cardiac cycle, and tube current reduction to 4% was applied outside the adjusted pulsing windows.

Contrast agent application was controlled by a bolus tracking technique. A region of interest was placed in the aortic root, and image acquisition started 7s after the signal density level reached the predefined threshold of 120 Hounsfield units (HU). For all CT examinations, a dual-head power injector (Stellant D; Medrad, Indianola, PA) was used to administer a three-phase bolus at a rate of 4.5 ml/s: first, 60–80 ml of undiluted contrast media (Iomeron 400, iomeprol, 400 mg/ml, Bracco, Milan, Italy) was administered. Thereafter, 45 ml of a 70%-to-30% blend of contrast medium and saline was administered. Finally, 45 ml of saline was administered.

A mono-segment reconstruction algorithm that uses the data from a full rotation of both detectors was used for image reconstruction. The data sets for the assessment of myocardial perfusion were reconstructed during the mid-diastolic phase, with reconstruction windows set at 60% to 75% of the R-R interval. For the reconstruction of axial images, we used a slice thickness of 0.75 mm and a slice increment of 0.4 m with dedicated dual-energy convolution kernel (D26f).

Cardiac MRI Among the 50 study participants, 36 underwent rest and stress-perfusion MRI. All MRI studies were performed with a 1.5-T whole-body system (Signa HD, GE Medical System, Milwaukee, WI) using an eight-element phased array surface coil (Cardiac coil, GE Medical Systems). Adenosine was administered intravenously using an automated power injector (MRidium, Iradimed, Winter Park, FL) at a constant rate of 140 μg/kg/min over 6 min

under continuous HR and blood pressure monitoring at 1-min intervals. After 4 min of the adenosine infusion, an intravenous bolus injection of 0.1 mmol/kg gadodiamide (Omniscan, GE Healthcare, Oslo, Norway) was injected into an antecubital vein on the opposite arm during an end-expiratory breath-hold. First-pass perfusion images were acquired every heart beat using a hybrid gradient echo/echo-planar pulse sequence (echo time 1.2 ms; flip angle 25°; slice thickness 8 mm; preparation pulse 90° for each slice; echo train length 4; field of view 36×36 cm; matrix 128×128; pixel size 0.28×0.28 cm) in three short-axis sections. Adenosine infusion was stopped after completion of the sequence. Ten minutes after the stress test, rest perfusion in the same orientation was performed using a second bolus of 0.1 mmol/kg gadodiamide.

Ten minutes after the second bolus, late enhancement (LE) images were acquired by using an inversion-recovery prepared gated fast-gradient echo-pulse sequence (repetition time 6.7 ms; echo time 3.3 ms; flip angle 25°; inversion time individually adjusted; slice thickness 8 mm; field of view 34×25.5 cm; matrix 128×96, matrix 256×160). Two long axes and five to six short axes were acquired.

CCA CCA (Allura Xper FD-10, Philips Medical Systems, Eindhoven, The Netherlands) was performed according to standard techniques and within 2–7 days after SP-MRI via the femoral or radial approach. A minimum of six projections was obtained: four views of the left and two of the right coronary artery. The segments were classified according to the 15-segment American Heart Association (AHA) model [15], which we modified by adding segment 16 for a ramus intermedius, when present.

Image interpretation

AIS-DECT AIS-DECT and cardiac MRI images were read by two independent radiologists (SM Ko, with 7 years of experience in cardiac imaging, and JW Choi, with 2 years of experience), blinded to the results of the other imaging tests. A consensus reading session was then performed to resolve any disagreements between both readers. DECT-based iodine maps were assessed for myocardial PDs using the AHA 17-segmental model [16], and three vascular territorial distributions were displayed using the dual-energy image postprocessing software of the Syngo-Multi-Modality Workplace (syngoDualEnergy, Siemens, Forchheim, Germany). Myocardial PDs on DECT-based iodine maps were defined as contiguous, circumscribed areas of decreased or absent iodine content within the LV myocardium, relative to remote normal myocardium [14]. To detect myocardial PDs, the DECT-based colour-coded iodine maps were superimposed onto grey-scale multiplanar reformation of the myocardium in the short- and long-axis views of the LV. Seventy percent overlay of the iodine map and the merged reconstruction with 5 mm-thick slap was used for the evaluation of myocardial perfusion. CT image quality was determined using a subjective three-point ranking scale: 1=poor, 2=good, 3=excellent.

Cardiac MRI MRI data were reviewed on an Advantage Windows workstation (GE Medical Systems). Image quality was graded on a scale between 1 and 3 (1=poor, 2=good, 3=excellent). Using visual assessment, myocardial perfusion was determined for every segment according to the AHA 17-segment model. AHA segment 17 corresponding to the apex was excluded from the analysis as it was not included in the standard short-axis views. Presence of hypo-enhancement in a coronary artery territory persisting for more than six heartbeats under adenosine stress was considered positive for PD and indicative of significant stenosis affecting the corresponding coronary artery [17].

LE images were analysed visually for the detection of hyperenhanced segments (infarcted myocardium) from subendocardium to epicardium. The distribution and pattern of LE was visually analysed in a 17-segment AHA model if LE was present.

CCA Quantitative assessment of stenosis severity on CCA was performed with a stenosis grading tool with automated distance and scale distance (CAAS, Pie Medical, Maastricht, The Netherlands). CCA studies were interpreted in consensus by two experienced cardiologists. Significant stenosis of the coronary artery was defined as the same as or more than 50% luminal narrowing compared with the expected diameter of the vessels in two orthogonal projections. Segments with a diameter of <1.5 mm were excluded from analysis because they usually do not constitute targets for revascularisation.

Radiation dose

Effective radiation dose for the DSCT (including calcium scoring and CTCA) and AIS-DECT examination was calculated in all patients. The dose-length product (DLP, measured in milligray-centimetres) is defined as the volume CT dose index multiplied by imaging length and is an indicator of the integrated radiation dose of the entire CT examination. DLP is displayed on the dose report on the CT and recoded. A reasonable approximation of the effective radiation dose of cardiac CT was calculated by multiplying DLP by a conversion coefficient for the chest ($\kappa=0.017\ \mathrm{mSv}\cdot\mathrm{mGy}^{-1}\cdot\mathrm{cm}^{-1}$) [18].

Statistical analysis

In the descriptive statistical analysis, quantitative variables were expressed as means ± standard deviations, and categorical variables were expressed as frequencies or percentages. With SP-MRI as the standard of reference, the diagnostic accuracy of AIS-DECT for the detection of reversible myocardial PDs was expressed in terms of the sensitivity, specificity, accuracy, positive predictive value (PPV) and negative predictive value (NPV). Compared with CCA, the diagnostic accuracy of AIS-DECT was assessed for the detection of vascular

territories with reversible myocardial PDs that were supplied by a significant coronary stenosis (≥50% lumen reduction).

Results

Study population All 50 patients completed the AIS-DECT protocol. Sixteen adverse events were reported in 13 patients; 8 patients complained of feeling flushed, 5 complained of headache, and 3 complained of chest discomfort. However, all of these events were transient and disappeared soon after the termination of adenosine infusion. Among the 50 patients, 9 patients were excluded from the study; 3 patients had old subendocardial MI detected by LE-MRI, 2 patients had poor CT image quality related to severely irregular HR, and 4 patients did not undergo CCA. Accordingly, 41 patients (25 men, mean age 64.1 years) were included in the study. The average effective radiation dose for the DSCT was 8.6± 1.6 mSv. Patients' characteristics are given in Table 1.

AIS-DECT AIS-DECT was completed for all 41 patients within 21.5±21.1 days of DSCT-CA imaging. With the use of adenosine, the average HR increased from 61± 8 bpm at rest to 70±11 bpm at stress. The average effective radiation dose for the AIS-DECT was 5.8± 0.6 mSv. Reversible myocardial PDs on AIS-DECT were found for 38 out of 41 patients (92.7%), 301 out of 697 myocardial segments (43.2%), and 72 out of 123 vascular territories (58.5%).

Cardiac MRI MRI data were analysed in 28 out of 36 patients because 5 patients were excluded in the study population and 3 patients had poor image quality related to breathing artefacts and dark rim artefacts. All 28 MRIs were of diagnostic image quality and obtained within 2.2± 0.9 days of AIS-DECT. On MRI, 25 out of 28 patients (89.3%), 185 out of 448 myocardial segments (41.3%) and 45 out of 84 vascular territories (53.6%) had reversible perfusion abnormalities.

Table 1 Clinical characteristics of 41 patients with angina

Characteristics	Data
Age (years)	64.1±9.1
Sex	25 men, 16 women
Heart rate (beats/min)	61±8
Weights (kg)	67±9.3
Body mass index (BMI) (kg/m^2)	27.2±2.4
Risk profile	
Diabetes	25
Hypertension	29
Hyperlipidemia	17
Obesity (BMI>30 kg/m^2)	8
Smoking	15
Current	9
Former	6
Treatment	
Coronary artery bypass graft	20
Percutaneous coronary intervention	6
Medication	15

CCA On CCA, 37 (90%) patients had significant stenosis, of whom 18 had significant stenosis in the right coronary artery territory, 30 in the left anterior descending artery territory and 17 in the left circumflex artery territory. Of these 37 patients, 15 (40.6%) patients had single-vessel disease, 14 (37.8%) had double-vessel disease and 8 (21.6%) had triple-vessel disease.

AIS-DECT and cardiac MRI Of the 222 segments with abnormal DECT stress perfusion, 164 were detected on SP-MRI (Figs. 1 and 2), but 58 were mismatched with SP-MRI (Fig. 3). Twenty-one segments with perfusion abnormalities on SP-MRI were mismatched with AIS-DECT. On a per-segment basis, AIS-DECT had a sensitivity of 89%, specificity of 79%, accuracy of 82%, PPV of 74% and NPV of 91% for the detection of segments with reversible myocardial PDs seen on SP-MRI. Of the 52 vascular territories with abnormal AIS-DECT perfusion, 41 were matched with SP-MRI, but 11 were not detected on SP-MRI. Four territories with reversible PDs on SP-MRI were not detected on AIS-DECT. On a per-vascular territory basis, ASI-DECT had a sensitivity of 91%, specificity of 72%, accuracy of 83%, PPV of 82% and NPV of 88% for the detection of vascular territories with reversible myocardial PDs (Table 2).

AIS-DECT and CCA Of the 72 vascular territories with reversible myocardial PDs, 58 had significant stenosis, but 14 were not related to significant stenosis on CCA. Seven vascular territories with significant CAD did not show perfusion abnormalities on AIS-DECT. AIS-DECT had a sensitivity of 89%, specificity of 76%, accuracy of 83%, PPV of 81% and NPV of 86% for the detection of vascular territories with ischaemic PDs that were supplied by a significant stenosis compared with CCA. Of the 38 patients with perfusion abnormalities, 36 had significant stenosis (Figs. 1, 2 and 3), but 2 did not have significant stenosis on CCA (Fig. 4). One patient with significant stenosis did not show reversible myocardial PD on AIS-DECT. On a per-patient basis, sensitivity for the classification of patients with or without haemodynamically relevant CAD using AIS-DECT was 97%, specificity was 50%, accuracy 93%, PPV was 95% and NPV was 95% in comparison with CCA.

Discussion

The results of our study indicate that AIS-DECT has feasibility and good diagnostic accuracy in detecting functionally relevant coronary stenoses causing stress-induced myocardial PDs in comparison with SP-MRI and CCA in patients with CAD.

CTCA usually does not provide myocardial perfusion information regarding the physiological significance of coronary stenosis because coronary flow is maintained

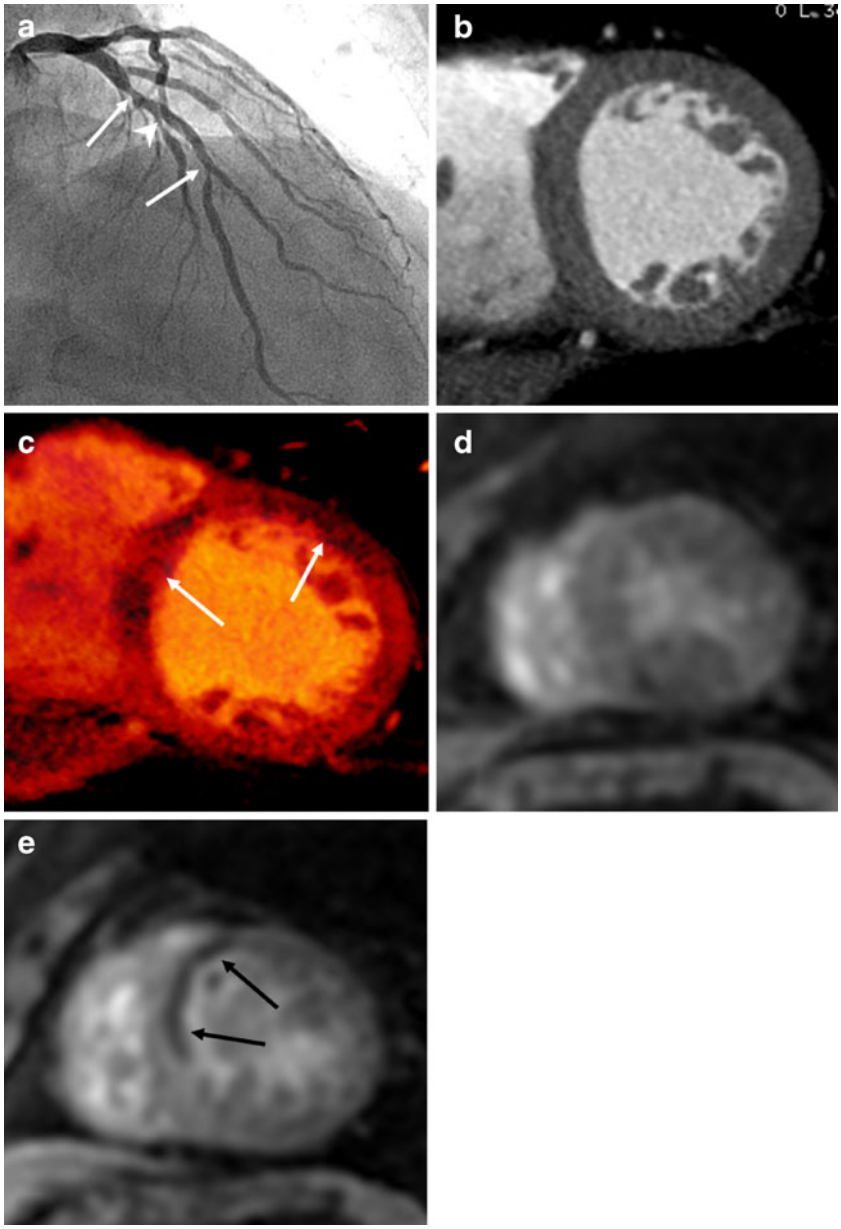

Fig. 1 Images of a 59-year-old man with chest pain. Conventional coronary angiogram (**a**) shows significant stenoses in the mid segment of the left anterior descending coronary artery (arrows) and third septal branch (arrowhead). The rest CT perfusion using dual-source CT (**b**) does not show any perfusion defects in the left ventricular (LV) myocardium. Dual-energy CT-based iodine map during adenosine infusion (**c**) reveals a perfusion defect in the mid anterior and anteroseptal LV myocardium (arrows). Findings are in good correlation with cardiac MRI acquired at rest (**d**) and stress (**e**), which reveal reversible subendocardial perfusion defect in the same myocardial areas (arrows)

until 80% stenosis [19–22]. AIS-MDCT studies in animal models have demonstrated that iodinated CT contrast agent has similar pharmacokinetics to gadolinium MRI contrast agents, that AIS-MDCT perfusion imaging correlates well with microsphere-derived myocardial blood flow and that ischaemic myocardial perfusion defects can be diagnosed by AIS-MDCT [6, 7]. With technological advances in CT including DSCT and wide-area detector CT, CT perfusion imaging can provide non-invasive coronary angiography and accurate assessment of myocardial perfusion at the same time, potentially serving as a "one-stop shop" [10, 23, 24]. Blankstein and colleagues reported that AIS-DSCT showed 93% sensitivity and 74% specificity for the detection of coronary stenosis (≥50% lumen reduction) with a corresponding SPECT perfusion abnormality [10].

With DSCT with dual-energy mode, an "iodine map" is created for the assessment of myocardial perfusion status by analysing iodine distribution within the myocardium based on the specific absorption characteristics of iodine for x-rays of high and low energy levels [11–14]. Ruzsics and colleagues showed that cardiac DECT without the administration of pharmacological stressors has the potential to allow detection of coronary artery stenosis and to provide the haemodynamic significance of the detected stenotic lesion on myocardial perfusion from a single examination [12, 14]. However, an iodine map contains a very broad range of iodine concentrations within the myocardium (normal variation in CT attenuation in different myocardial areas) and may be influenced by several factors such as normalisation of the iodine to areas of normal myocardial perfusion, beam hardening artefacts

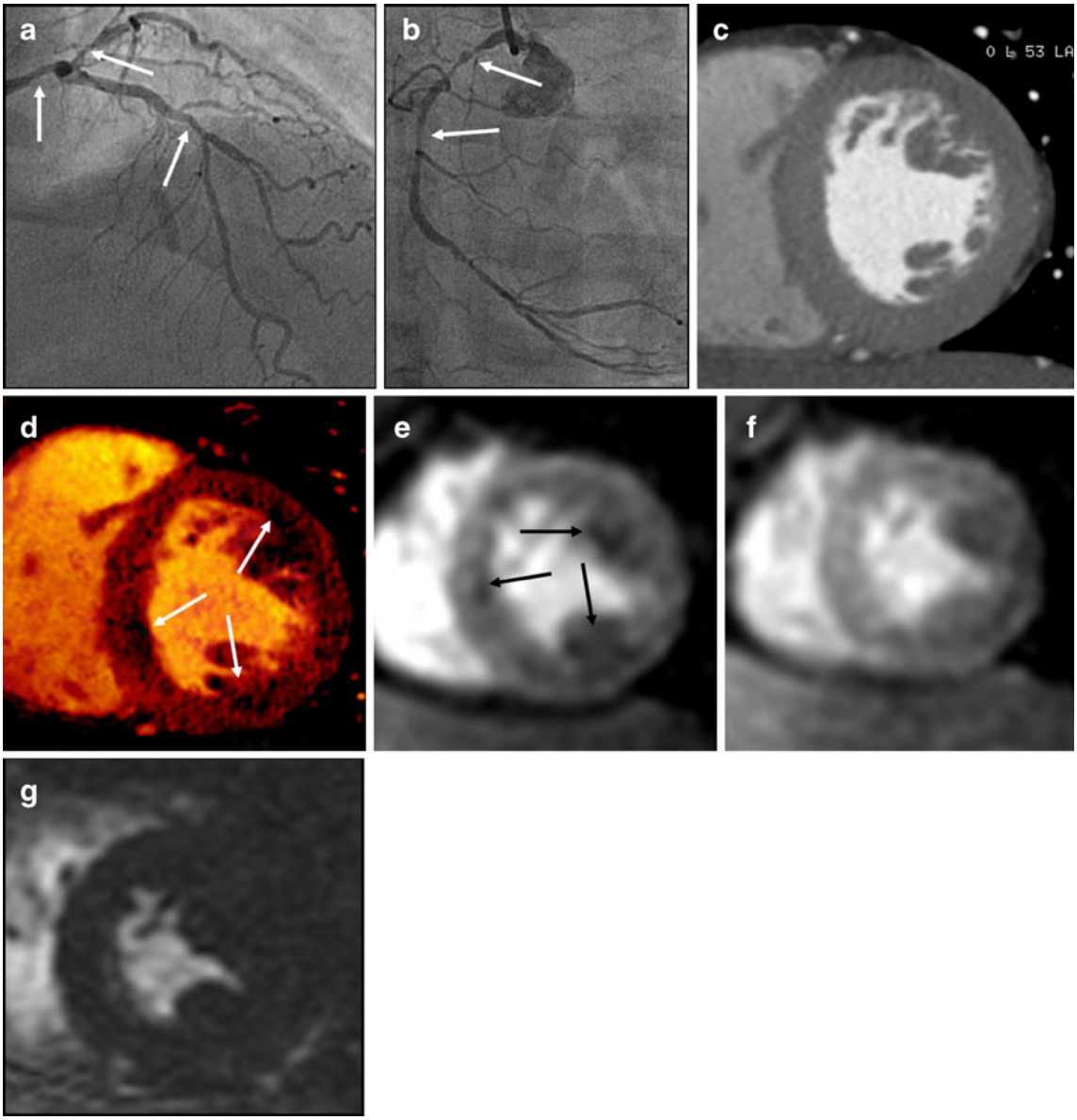

Fig. 2 Images of a 55-year-old woman with angina. Conventional coronary angiography shows significant stenosis (arrows) in the left main, mid segment of the left anterior descending and the proximal segment of the left circumflex coronary arteries (**a**) and proximal segment of the right coronary artery (**b**). The CT perfusion image at rest (**c**) does not show any perfusion defects in the left ventricular (LV) myocardium. Dual-energy CT-based iodine map during adenosine infusion (**d**) reveals a concentric perfusion defect in the mid LV myocardium. Findings are in good correlation with cardiac MRI acquired at rest (**e**) and stress (**f**), which reveals reversible subendocardial perfusion defect in the same myocardial areas. Delayed-enhanced cardiac MRI (**g**) does not show any delayed enhancement along the mid LV myocardium

and cardiac motion artefact [6, 13, 25, 26]. In addition, AIS-CT perfusion imaging is more physiologically acceptable and feasible than DECT at rest in detecting reversible myocardial ischaemia because adenosine increases the difference in myocardial perfusion between ischaemic and normally perfused myocardium [27].

We hypothesised that adenosine stress DECT-based iodine mapping might be sensitive for the detection of haemodynamically significant stenosis causing reversible myocardial PD because of combined application of DECT and AIS-CT perfusion imaging. In the study, a total of 448 segments were compared, and 164 segments were both AIS-DECT and SP-MRI perfusion positive. The agreement of perfusion between two modalities was 74%. An excellent correlation between DSCT and SPECT at rest and under stress was shown for the detection of perfusion abnormalities and for the assessment of PD severity on a per-segment, per-vessel and per-patient basis [28]. Even though SPECT is an established clinical standard for the detection of myocardial PDs in patients with CAD, we used SP-MRI as the reference standard for perfusion measurement because of higher spatial resolution over

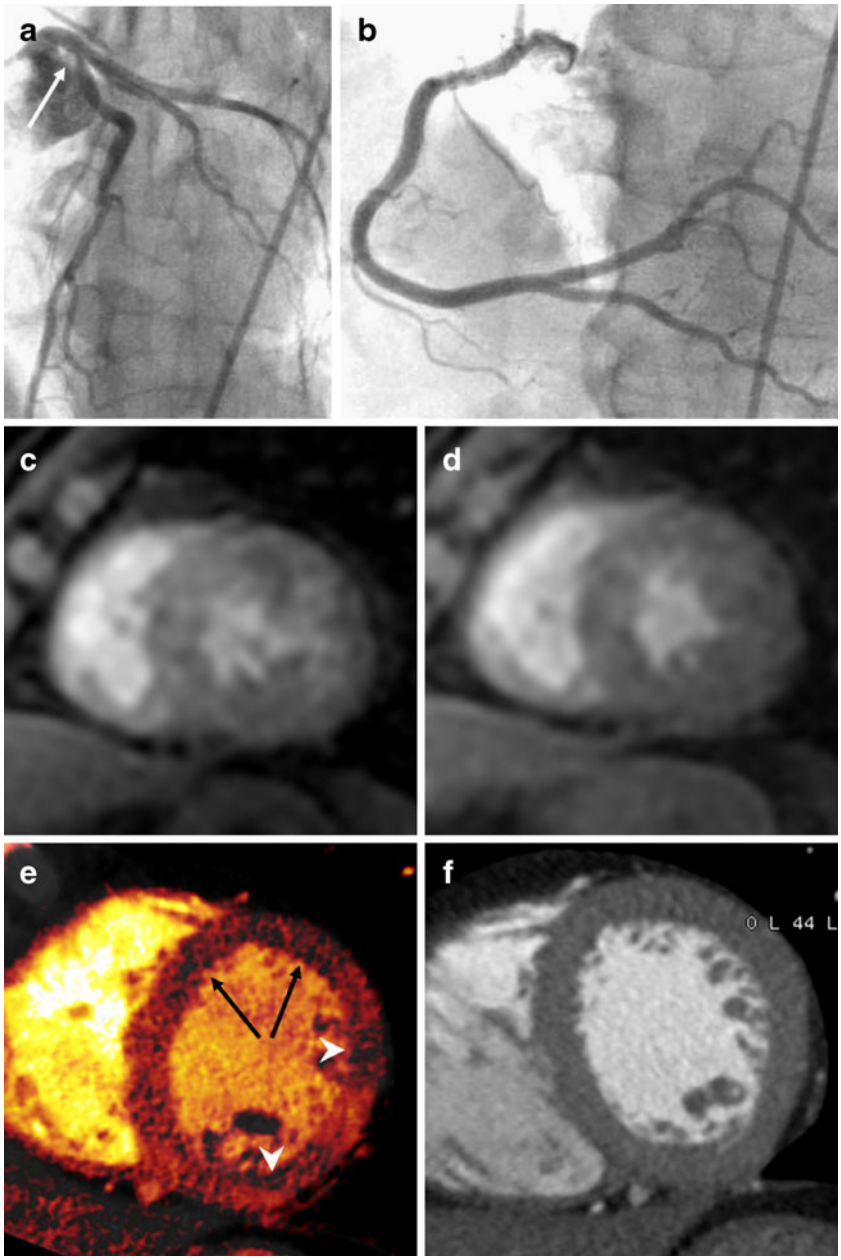

Fig. 3 Images of a 58-year-old man with angina. Conventional coronary angiography shows severe stenosis (arrow) in the ostium of left anterior descending coronary artery (**a**), but no significant stenoses in the right coronary artery (**b**). Cardiac MRIs acquired at stress (**c**) and rest (**d**) do not show any perfusion defects in the left ventricular (LV) myocardium. Dual-energy CT-based iodine map during adenosine infusion (**e**) reveals transmural perfusion defects in the mid-anterior and anteroseptal LV myocardium (arrows) and patchy perfusion defects in the inferior and anterolateral LV myocardium (arrowheads). The rest CT perfusion using dual-source CT (**f**) does not show any perfusion defects in the LV myocardium. The false-positive finding in the mid inferior and anterolateral LV wall is related to the heterogeneous areas of normal myocardial perfusion

SPECT and no radiation exposure. It should be noted that CT perfusion is vulnerable to beam hardening and cardiac motion artefacts, leading to degradation of overall image quality and false-positive findings. Specifically, AIS-DECT perfusion is more susceptible to these CT artefacts than AIS-DSCT perfusion due to poor temporal resolution of 330 ms and heterogeneous areas of normal myocardial perfusion. In our study, 58 segments of false-positive PD were related to CT artefacts and commonly located in the apical anterior and basal inferior wall. By the same token, AIS-DECT had 14 false-positive territories that were not supplied by a significant stenosis in comparison with CCA. Despite the limitations hampering AIS-DECT's ability to assess myocardial perfusion and coronary stenosis simultaneously, AIS-DECT has the potential to detect myocardial perfusion abnormalities more sensitively and accurately than stress single-energy CT. This is probably because AIS-DECT provides three different energy images (low kV, high kV and merged images) and an iodine map at the same time. However, further studies are required to determine the diagnostic value of AIS-DECT compared with stress single-energy CT and other clinical reference standards, particularly SP-MRI.

Our study contains several significant limitations:

1. This study was a single-institution study, and the number of patients was relatively small. Thus, a blinded, prospective, randomised multicentre study in a large population needs to be performed for further validation of the use of AIS-DECT.
2. Whilst our study was a prospective study, cardiac MRI was performed in 28 patients. Cardiac MRI might not

Table 2 Performance characteristics of stress DECT

	Stress DECT performance characteristics				
	Sensitivity	Specificity	Accuracy	PPV	NPV
Cardiac MRI (n=28)					
Segment	0.89	0.78	0.82	0.74	0.91
Territory	0.91	0.72	0.83	0.82	0.88
CCA (n=41)					
Territory	0.89	0.76	0.83	0.81	0.86
Patient	0.97	0.5	0.93	0.95	0.67

DECT, dual-energy computed tomography; MRI, magnetic resonance imaging; CCA, conventional coronary angiography; PPV, positive predictive value; NPV, negative predictive value

be an adequate reference standard for perfusion measurements in the study.

3. This study design is prone to selection and verification bias. Given the known CAD in this group, most patients were likely to have myocardial perfusion abnormalities on MPI. As such, many patients (25/28, 89.3%) had true-positive PDs on both modalities. This might result in false positives on both modalities. The applicability of the study results in patients with intermediate pretest probability of CAD is uncertain.
4. The 330-ms temporal resolution of DECT utilised by the AIS-DECT protocol was closely related to reduction of image quality for MPI because of susceptibility to cardiac motion artefacts during adenosine infusion.
5. Beam-hardening artefacts closely resembled a myocardial PD and led to false positives on AIS-DECT.
6. AIS-DECT is a newly introduced imaging technique, so there is no documented optimal imaging protocol (amount and speed of contrast administration, imaging delay time, etc.) and imaging postprocessing technique to normalise iodine in the iodine map to areas of normal myocardial perfusion.
7. The study was designed to assess only myocardial perfusion. Therefore, this method may not allow for

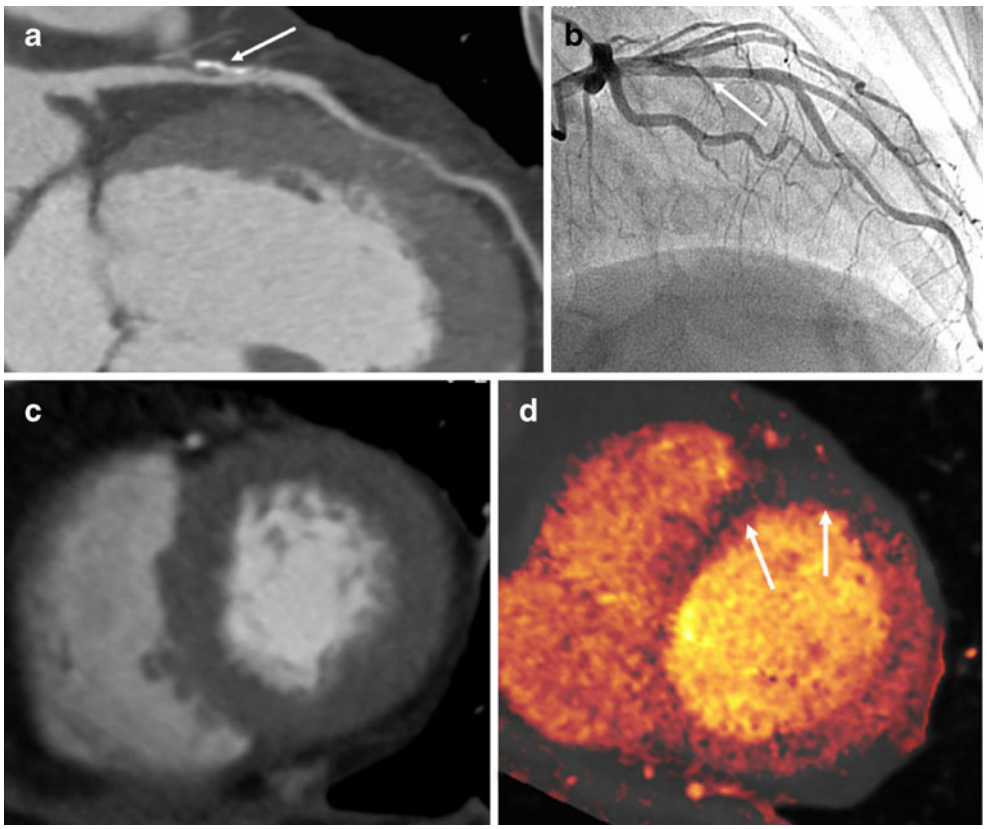

Fig. 4 Images in a 66-year-old man with dyspnea and chest pain. Coronary CT angiography (**a**) shows moderate stenosis with mixed calcified and non-calcified plaque in the proximal segment of the left anterior descending (LAD) coronary artery (arrow). Conventional coronary angiogram (**b**) does not reveal significant stenosis in the corresponding segment of LAD (arrow). The rest CT perfusion using dual-source CT (**c**) does not show any perfusion defects in the left ventricular (LV) myocardium. Dual-energy CT-based iodine map during adenosine infusion (**d**) reveals a perfusion defect in the apical anterior and anteroseptal LV myocardium (arrows). The false-positive finding in the apical anterior and anteroseptal LV wall is related to the beam-hardening artefact

visualisation of the coronary arteries during adenosine infusion.

8. Radiation exposure to patients with the use of the applied protocol is still considerable even though radiation exposure with AIS-DECT was 5.8 mSv and was lower than the recently reported stress SPECT (9.2 mSv) [28]. However, the average total radiation exposure for the DSCT (calcium score and CTCA) and AIS-DECT was 14.5±1.8 mSv and higher than DSCT stress and rest perfusion (12.3±4.3 mSv) and SPECT (12.4±1.9 mSv) [28]. AIS-DECT might not be practical in routine clinical practice because radiation and iodinated contrast media should be used, and SP-MRI is the emerging reference standard for detection of myocardial perfusion abnormalities. However, AIS-DECT has been suggested as an attractive alternative to standard SP-MRI and SPECT for the detection of CAD considering its relatively low radiation exposure, simple study protocol, short examination time, high spatial resolution and applicability to patients with cardiac MRI contraindications.

Despite these important limitations, our initial experience of AIS-DECT demonstrated feasibility and good diagnostic accuracy in detecting functionally relevant coronary stenoses causing stress-induced myocardial PDs in comparison to SP-MRI and CCA in patients with known CAD. AIS-DECT has the potential to become a promising imaging technique for the evaluation of myocardial perfusion and can be used as an alternative to other MPI techniques. However, we recommend cautious clinical application of the results to low CAD prevalence populations. Larger multicentre studies are required to explore the growing value of this imaging technique.

Acknowledgements This work was supported by Konkuk University in 2010. The authors would like to thank the CT and MR technologists, the radiology department nursing staff, the cardiology department staff physicians and the residents in the Division of Thoracic Surgery at the Konkuk University Hospital.

References

1. Nesto RW, Kowalchuk GJ (1987) The ischemic cascade: temporal sequence of hemodynamic, electrocardiographic and symptomatic expressions of ischemia. Am J Cardiol 59:23C–30C
2. Leong-Poi H, Rim SJ, Le DE, Fisher NG, Wei K, Kaul S (2002) Perfusion versus function: the ischemic cascade in demand ischemia: implication of single-vessel versus multivessel stenosis. Circulation 105:987–992
3. Hachamovitch R, Berman DS, Kiat H, Cohen I, Cabico JA, Friedman J et al (1996) Exercise myocardial perfusion SPECT in patients without known coronary artery disease: incremental prognostic value and use in risk stratification. Circulation 93:905–914
4. Schwitter J, Nanz D, Kneifel S, Berschinger K, Buchi M, Knusel PR et al (2001) Assessment of myocardial perfusion in coronary artery disease by magnetic resonance: a comparison with positron emission tomography and coronary angiography. Circulation 103:2230–2235
5. Kurata A, Mochizuki T, Koyama Y, Haraikawa T, Suzuki J, Shigematsu Y et al (2005) Myocardial perfusion imaging using adenosine triphosphate stress multi-slice spiral computed tomography: alternative to stress myocardial perfusion scintigraphy. Circ J 69:550–557
6. George RT, Silva C, Cordeiro MA, DiPaula A, Thompson DR, McCarthy WF et al (2006) Multidetector computed tomography myocardial perfusion imaging during adenosine stress. J Am Coll Cardiol 48:153–160
7. George RT, Jerosch-Herold M, Silva C, Kitagawa K, Bluemke DA, Lima JA et al (2007) Quantification of myocardial perfusion using dynamic 64-detector computed tomography. Invest Radiol 42:815–822
8. Kido T, Kurata A, Higashino H, Inoue Y, Kanza RE, Okayama H et al (2008) Quantification of regional myocardial blood flow using first-pass multidetector-row computed tomography and adenosine triphosphate in coronary artery disease. Circ J 72:1086–1091
9. Petersilka M, Bruder H, Krauss B, Stierstorfer K, Flohr TG (2008) Technical principles of dual source CT. Eur J Radiol 68:362–368
10. Blankstein R, Shturman LD, Rogers IS, Rocha-Filho JR, Okada DR, Sarwar A et al (2009) Adenosine-induced stress myocardial perfusion imaging using dual-source cardiac computed tomography. J Am Coll Cardiol 54:1072–1084
11. Johnson TR, Krauss B, Sedlmair M, Grasruck M, Bruder H, Morhard D et al (2007) Material differentiation by dual energy CT: initial experience. Eur Radiol 17:1510–1517
12. Ruzsics B, Lee H, Zwerner PL, Gebregziabher M, Costello P, Schoepf UJ (2008) Dual-energy CT of the heart for diagnosing coronary artery stenosis and myocardial ischemia-initial experience. Eur Radiol 18:2414–2424
13. Schwarz F, Ruzsics B, Schoepf UJ, Bastarrika G, Chiaramida SA, Abro JA et al (2008) Dual-energy CT of the heart-principles and protocols. Eur J Radiol 68:423–433
14. Ruzsics B, Schwarz F, Schoepf UJ, Lee YS, Bastarrika G, Chiaramida SA et al (2009) Comparison of dual-energy computed tomography of the heart with single photon emission computed tomography for assessment of coronary artery stenosis and of the myocardial blood supply. Am J Cardiol 104:318–326
15. Austen WG, Edwards JE, Frye RL, Gensini GG, Gott VL, Griffith LS et al (1975) A reporting system on patients evaluated for coronary artery disease. Report of the AD Hoc Committee for Grading of Coronary Artery disease, Council on Cardiovascular Surgery, American Heart Association. Circulation 51(4 Suppl):5–40
16. Cerqueira MD, Weissman NJ, Dilsizian V, Jacobs AK, Kaul S, Laskey WK et al (2002) Standardized myocardial segmentation and nomenclature for tomographic imaging of the heart: a statement for healthcare professionals from the Cardiac Imaging Committee of the Council on Clinical Cardiology of the American Heart Association. Circulation 105:539–542

17. Pilz G, Klos M, Ali E, Hoefling B, Scheck R, Bernhardt P (2008) Angiographic correlations of patients with small vessel disease diagnosed by adenosine-stress cardiac magnetic resonance imaging. J Cardiovasc Magn Reson 10:8
18. Morin RL, Gerber TC, McCollough CH (2003) Radiation dose in computed tomography of the heart. Circulation 107:917–922
19. Gould KL, Lipscomb K (1974) Effects of coronary stenoses on coronary flow reserve and resistance. Am J Cardiol 34:48–55
20. Sato A, Hiroe M, Tamura M, Ohigashi H, Nozato T, Hikita H et al (2008) Quantitative measures of coronary stenosis severity by 64-slice CT angiography and relation to physiologic significance of perfusion in nonobese patients: comparison with stress myocardial perfusion imaging. J Nucl Med 49:564–572
21. Gaemperli O, Schepis T, Valenta I, Koepfli P, Husmann L, Scheffel H et al (2008) Functionally relevant coronary artery disease: comparison of 64-section CT angiography with myocardial perfusion SPECT. Radiology 248:414–423
22. Santana CA, Garcia EV, Faber TL, Sirineni GK, Esteves FP, Sanyal R et al (2009) Diagnostic performance of fusion of myocardial perfusion imaging (MPI) and computed tomography coronary angiography. J Nucl Cardiol 16:201–211
23. George RT, Arbab-Zadeh A, Miller JM, Kitagawa K, Chang HJ, Bluemke DA et al (2009) Adenosine stress 64- and 256-row detector computed tomography angiography and perfusion imaging: a pilot study evaluating the transmural extent of perfusion abnormalities to predict atherosclerosis causing myocardial ischemia. Circ Cardiovasc Imaging 2:174–182
24. Rocha-Filho JA, Blankstein R, Shturman LD, Bezerra HG, Okada DR, Rogers IS et al (2010) Incremental value of adenosine-induced stress myocardial perfusion imaging with dual-source CT at cardiac CT angiography. Radiology 254:410–419
25. Blankstein R, Okada DR, Rocha-Filho JA, Rybicki FJ, Brady TJ, Cury RC (2009) Cardiac myocardial perfusion imaging using dual source computed tomography. Int J Cardiovasc Imaging 25:209–216
26. Rodriguez-Granillo GA, Rosales MA, Degrossi E, Rodriguez AE (2010) Signal density of left ventricular myocardial segments and impact of beam hardening artifact: implications for myocardial perfusion assessment by multidetector CT coronary angiography. Int J Cardiovasc Imaging 26:345–354
27. Verani MS (1991) Pharmacological stress with adenosine for myocardial perfusion imaging. Semin Nucl Med 21:266–272
28. Okada DR, Ghoshhajra BB, Blankstein R, Rocha-Filho JR, Shturman LD, Rogers IS et al (2010) Direct comparison of rest and adenosine stress myocardial perfusion CT with rest and stress SPECT. J Nucl Cardiol 17:27–37